Available online at www.sciencedirect.com
ScienceDirect
Publishing Services by Elsevier
International Journal of Naval Architecture and Ocean Engineering xx (2016) 1–17
http://www.journals.elsevier.com/international-journal-of-naval-architecture-and-ocean-engineering/

A second order analytical solution of focused wave group interacting with a vertical wall

Yonggang Sun [a], Xiantao Zhang [b,*]

[a] Wuxi First Scientific Research Institute, Wuxi, PR China
[b] Center for Offshore Foundation Systems, The University of Western Australia, WA 6009, Australia

Received 16 May 2016; revised 18 August 2016; accepted 4 September 2016
Available online ■ ■ ■

Abstract

The interaction of focused wave groups with a vertical wall is investigated based on the second order potential theory. The NewWave theory, which represents the most probable surface elevation under a large crest, is adopted. The analytical solutions of the surface elevation, velocity potential and wave force exerted on the vertical wall are derived, up to the second order. Then, a parametric study is made on the interaction between nonlinear focused wave groups and a vertical wall by considering the effects of angles of incidence, wave steepness, focal positions, water depth, frequency bandwidth and the peak lifting factor. Results show that the wave force on the vertical wall for obliquely-incident wave groups is larger than that for normally-incident waves. The normalized peak crest of wave forces reduces with the increase of wave steepness. With the increase of the distance of focal positions from the vertical wall, the peak crest of surface elevation, although fluctuates, decreases gradually. Both the normalized peak crest and adjacent crest and trough of wave forces become larger for shallower water depth. For focused wave groups reflected by a vertical wall, the frequency bandwidth has little effects on the peak crest of wave elevation or forces, but the adjacent crest and trough become smaller for larger frequency bandwidth. There is no significant change of the peak crest and adjacent trough of surface elevation and wave forces for variation of the peak lifting factor. However, the adjacent crest increases with the increase of the peak lifting factor.

Keywords: Second order; Focused wave groups; NewWave; Vertical wall; Interaction

1. Introduction

The interaction of sea waves with a vertical wall is a classic problem in coastal engineering. With the assumption of full reflection, such an interaction leads to the formation of standing waves. Traditionally, the random sea environment is usually simplified as a deterministic, monochromatic and periodic regular waves with the height and period assumed to correspond to the extreme sea conditions. As a result, early studies on the interaction of waves with a vertical wall (or equivalently standing waves) focused on periodic regular waves. Rayleigh (1915) gave a third order solution of two dimensional standing waves in infinite water depth, which was further extended to the fifth order by Penney and Price (1952). Standing waves in finite water depth was investigated by Tadjbakhsh and Keller (1960), up to the third order, and extended to the fourth order by Goda (1967). Accompanied by numerical approaches, some experimental work was also carried out by researchers to either validate the numerical methods or provide a deeper understanding of both kinematic and dynamic properties of standing waves (Taylor, 1953; Fultz, 1962; Edge and Walters, 1964).

However, the regular wave representation of a random sea state is unrealistic, especially for extreme events emerging in the random process. In a stationary Gaussian random wave field, the statistically averaged wave profile under a crest is represented by NewWave theory (Tromans et al., 1991) or equivalently by Quasi-Determinism (QD) theory (Boccotti,

* Corresponding author.
E-mail address: zhxter@outlook.com (X. Zhang).
Peer review under responsibility of Society of Naval Architects of Korea.

http://dx.doi.org/10.1016/j.ijnaoe.2016.09.002

1997a). The concept is to generate an extreme wave at a specified position and time through the superposition of relatively small amplitude waves of different frequencies (i.e. focused wave groups). These wave theories include much of the spectral properties of the sea state and in the meanwhile they are time saving compared with traditional time domain simulation of random irregular waves. By using the second order Stokes expansion given by Sharma and Dean (1981) and Dalzell (1999), the NewWave theory or QD theory was extended to the second order for focused wave groups in undisturbed wave field (Walker et al., 2004; Arena, 2005; Fedele and Arena, 2005; Arena et al., 2008). Experimental research was also conducted by researchers to investigate the kinematics and energy transfer during the evolution of focused wave groups (Baldock and Swan, 1996; Sriram et al., 2015).

With the development of these wave theories, the interaction of focused wave groups with a vertical wall was further investigated by researchers. Boccotti (1997b) applied the QD theory to derive the first order analytic solution for the case of both long-crested and short-crested waves in front of a wall. The results was validated by a small-scale field experiment (Boccotti et al., 1993). Prabhakar and Sundar (2001) investigated the pressure exerted by standing waves on a vertical wall. Romolo and Arena (2008) gave an analytical solution for the second order free surface displacement and velocity potential when a high crest of long-crested (two-dimensional) waves occurs at some fixed point on or close to a vertical wall. With the analytical solution, the space and time evolution and the effects of finite water depth on the evolution were discussed in detail. This work was extended by Romolo and Arena (2013) and Romolo et al. (2014) to short-crested (three dimensional) wave groups in front a vertical wall. The second order analytical solutions mentioned above (for both two and three dimensional wave groups, Romolo and Arena, 2008; Romolo and Arena, 2013; Romolo et al., 2014) actually gave the averaged wave profile under a large crest of the underlying standing wave field (First a standing wave field is formed and then the QD theory is used to obtain the averaged wave profile under a large crest in the standing wave field). The problem (the interaction of focused wave groups with a vertical wall) may also be investigated from a different point of view. First, an undisturbed focused wave group focuses at a given position at a given time (i.e. a large crest occurs at this undisturbed wave field). Then the focused wave groups meet a vertical wall and are fully reflected.

In the present paper, the interaction of nonlinear focused wave groups with a vertical wall is investigated based on the second order potential theory. NewWave theory, correct to second order, is adopted in this study. Analytical solutions of both surface elevation and velocity potential, as well as wave forces exerted on the vertical wall are derived. Then a parametric study is made on the surface elevation and wave forces by considering the effects of angle of incidence, wave steepness, focal position, water depth, frequency bandwidth and peak lifting factor.

2. Governing equations

A sketch of the fluid domain where waves interact with a vertical wall is shown in Fig. 1. The water depth for the fluid domain is denoted as h. An x, y, z Cartesian coordinate system (satisfying the right hand rule) is applied to define the locations, with the origin located on the undisturbed equilibrium surface. The z coordinate is vertical and positive upwards. In the horizontal $x-y$ plane, the x axis is pointed normally toward the vertical wall and the y coordinate is parallel to the vertical wall. The fluid is assumed to be inviscid and incompressible. The fluid motion is assumed to be irrotational. Based on the assumption, the velocity field, $\vec{u}$, can be defined by a potential function, ϕ, i.e. $\vec{u} = \nabla\phi$, which satisfies

$$\nabla^2\phi = 0 \tag{1}$$

in the fluid domain. And at the bottom of the fluid domain, the velocity potential satisfies the condition as follows,

$$\frac{\partial\phi}{\partial z} = 0 \quad \text{on } z = -h \tag{2}$$

The dynamic boundary condition on the free surface is:

$$g\eta + \frac{\partial\phi}{\partial t} + \frac{1}{2}\left[\left(\frac{\partial\phi}{\partial x}\right)^2 + \left(\frac{\partial\phi}{\partial y}\right)^2 + \left(\frac{\partial\phi}{\partial z}\right)^2\right] = 0 \quad \text{on } z = \eta \tag{3}$$

with the assumption of zero atmospheric pressure on the free surface. And the kinematic boundary condition on the free surface is given as follows,

$$\frac{\partial\eta}{\partial t} - \frac{\partial\phi}{\partial z} + \frac{\partial\phi}{\partial x}\frac{\partial\eta}{\partial x} + \frac{\partial\phi}{\partial y}\frac{\partial\eta}{\partial y} = 0 \quad \text{on } z = \eta \tag{4}$$

It can be found from Eq. (3) and Eq. (4) that the unknown velocity potential is defined on the unknown free surface. In order to solve the problem, the technique of Taylor series expansion (Newman, 1977) is used to expand both the kinematic and dynamic boundary conditions on the equilibrium free surface $z = 0$, up to pre-determined order. As a result, the approximate dynamic and kinematic free surface boundary conditions to be satisfied, correct to second order, are given as follows,

$$g\eta + \frac{\partial\phi}{\partial t} + \eta\frac{\partial^2\phi}{\partial z\partial t} + \frac{1}{2}\left[\left(\frac{\partial\phi}{\partial x}\right)^2 + \left(\frac{\partial\phi}{\partial y}\right)^2 + \left(\frac{\partial\phi}{\partial z}\right)^2\right] = 0 \quad \text{on } z = 0 \tag{5}$$

$$\frac{\partial\eta}{\partial t} - \left(\frac{\partial\phi}{\partial z} + \eta\frac{\partial^2\phi}{\partial z^2}\right) + \frac{\partial\phi}{\partial x}\frac{\partial\eta}{\partial x} + \frac{\partial\phi}{\partial y}\frac{\partial\eta}{\partial y} = 0 \quad \text{on } z = 0 \tag{6}$$

Also the velocity potential needs to satisfy the boundary condition at the vertical wall, i.e.

$$\frac{\partial\phi}{\partial x} = 0 \quad \text{on } x = x_1 \tag{7}$$

Please cite this article in press as: Sun, Y., Zhang, X., A second order analytical solution of focused wave group interacting with a vertical wall, International Journal of Naval Architecture and Ocean Engineering (2016), http://dx.doi.org/10.1016/j.ijnaoe.2016.09.002

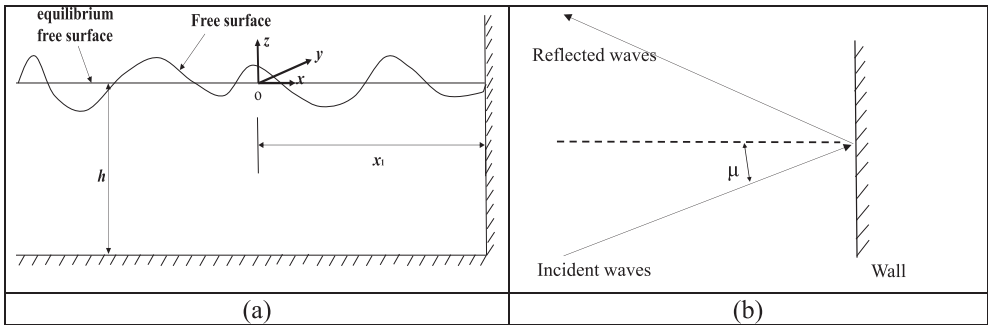

Fig. 1. A sketch of the fluid domain where waves interact with a vertical wall: (a) front view; (b) top view.

Eqs. (1), (2) and (5)–(7) are the governing equations for nonlinear waves interacting with a vertical wall, correct to second order.

3. Derivation of relevant expressions

First, we consider about second order wave–wave interaction without the vertical wall in the fluid domain. According to Sharma and Dean (1981) or Dalzell (1999), the solution to second order interactions between two linear waves is given as follows,

$$\begin{aligned}\eta=&\sum_{i=1}^{2}a_i\cos\psi_i+a_1a_2B_{12}^{+}\cos(\psi_1+\psi_2)\\&+a_1a_2B_{12}^{-}\cos(\psi_1-\psi_2)\\&+\sum_{i=1}^{2}\frac{a_i^2|\overrightarrow{k}_i|}{4\tanh(|\overrightarrow{k}_i|h)}\left(2+\frac{3}{\sinh^2(|\overrightarrow{k}_i|h)}\right)\cos(2\psi_i)\\&-\sum_{i=1}^{2}\frac{a_i^2|\overrightarrow{k}_i|}{2\sinh(2|\overrightarrow{k}_i|h)}\end{aligned}\tag{8}$$

$$\begin{aligned}\phi=&\sum_{i=1}^{2}a_i\frac{g}{\omega_i}\frac{\cosh\{|\overrightarrow{k}_i|(z+h)\}}{\cosh(|\overrightarrow{k}_i|h)}\sin\psi_i\\&+\sum_{i=1}^{2}a_i^2\frac{3}{8}\omega_i\frac{\cosh\{2|\overrightarrow{k}_i|(z+h)\}}{\sinh^4(|\overrightarrow{k}_i|h)}\sin(2\psi_i)\\&+a_1a_2A_{12}^{+}\frac{\cosh\{|\overrightarrow{k}_1+\overrightarrow{k}_2|(z+h)\}}{\cosh(|\overrightarrow{k}_1+\overrightarrow{k}_2|h)}\sin(\psi_1+\psi_2)\\&+a_1a_2A_{12}^{-}\frac{\cosh\{|\overrightarrow{k}_1-\overrightarrow{k}_2|(z+h)\}}{\cosh(|\overrightarrow{k}_1-\overrightarrow{k}_2|h)}\sin(\psi_1-\psi_2)\end{aligned}\tag{9}$$

where g is the acceleration of gravity, h is the water depth, a_i, ω_i and $\overrightarrow{k}_i$ are, respectively, the amplitude, circular frequency and the vector wave number of the ith (i = 1, 2) wave component. $\psi_i=\overrightarrow{k}_i\cdot\overrightarrow{X}-\omega_i t+\varepsilon_i$ is the phase function of the ith wave component, with $\overrightarrow{X}$ being the position vector in the x–y plane and ε_i denoting an arbitrary constant phase.

The components of the interaction kernels A_{ij}^{+}, A_{ij}^{-}, B_{ij}^{+}, B_{ij}^{-}, D_{ij}^{+} and D_{ij}^{-} are defined as

$$\begin{aligned}A_{12}^{+}=&-\frac{\omega_1\omega_2(\omega_1+\omega_2)}{D_{12}^{+}}\left(1-\frac{\cos(\mu_1-\mu_2)}{\tanh(|\overrightarrow{k}_1|h)\tanh(|\overrightarrow{k}_2|h)}\right)\\&+\frac{1}{2D_{12}^{+}}\left(\frac{\omega_1^3}{\sinh^2(|\overrightarrow{k}_1|h)}+\frac{\omega_2^3}{\sinh^2(|\overrightarrow{k}_2|h)}\right)\end{aligned}\tag{10}$$

$$\begin{aligned}A_{12}^{-}=&\frac{\omega_1\omega_2(\omega_1-\omega_2)}{D_{12}^{-}}\left(1+\frac{\cos(\mu_1-\mu_2)}{\tanh(|\overrightarrow{k}_1|h)\tanh(|\overrightarrow{k}_2|h)}\right)\\&+\frac{1}{2D_{12}^{-}}\left(\frac{\omega_1^3}{\sinh^2(|\overrightarrow{k}_1|h)}-\frac{\omega_2^3}{\sinh^2(|\overrightarrow{k}_2|h)}\right)\end{aligned}\tag{11}$$

$$\begin{aligned}B_{12}^{+}=&\frac{\omega_1^2+\omega_2^2}{2g}-\frac{\omega_1\omega_2}{2g}\left(1-\frac{\cos(\mu_1-\mu_2)}{\tanh(|\overrightarrow{k}_1|h)\tanh(|\overrightarrow{k}_2|h)}\right)\\&\times\frac{(\omega_1+\omega_2)^2+g|\overrightarrow{k}_1+\overrightarrow{k}_2|\tanh(|\overrightarrow{k}_1+\overrightarrow{k}_2|h)}{D_{12}^{+}}\\&+\frac{\omega_1+\omega_2}{2gD_{12}^{+}}\left(\frac{\omega_1^3}{\sinh^2(|\overrightarrow{k}_1|h)}+\frac{\omega_2^3}{\sinh^2(|\overrightarrow{k}_2|h)}\right)\end{aligned}\tag{12}$$

$$\begin{aligned}B_{12}^{-}=&\frac{\omega_1^2+\omega_2^2}{2g}+\frac{\omega_1\omega_2}{2g}\left(1+\frac{\cos(\mu_1-\mu_2)}{\tanh(|\overrightarrow{k}_1|h)\tanh(|\overrightarrow{k}_2|h)}\right)\\&\times\frac{(\omega_1-\omega_2)^2+g|\overrightarrow{k}_1-\overrightarrow{k}_2|\tanh(|\overrightarrow{k}_1-\overrightarrow{k}_2|h)}{D_{12}^{-}}\\&+\frac{\omega_1-\omega_2}{2gD_{12}^{-}}\left(\frac{\omega_1^3}{\sinh^2(|\overrightarrow{k}_1|h)}-\frac{\omega_2^3}{\sinh^2(|\overrightarrow{k}_2|h)}\right)\end{aligned}\tag{13}$$

$$D_{12}^{+}=(\omega_1+\omega_2)^2-g|\overrightarrow{k}_1+\overrightarrow{k}_2|\tanh(|\overrightarrow{k}_1+\overrightarrow{k}_2|h)\tag{14}$$

Please cite this article in press as: Sun, Y., Zhang, X., A second order analytical solution of focused wave group interacting with a vertical wall, International Journal of Naval Architecture and Ocean Engineering (2016), http://dx.doi.org/10.1016/j.ijnaoe.2016.09.002

$$D_{12}^{-} = (\omega_1 - \omega_2)^2 - g\left|\overrightarrow{k}_1 - \overrightarrow{k}_2\right| tanh\left(\left|\overrightarrow{k}_1 - \overrightarrow{k}_2\right| h\right) \tag{15}$$

where, $\mu_i (i = 1, 2)$ is the direction of propagation in the horizontal $x-y$ plane for the ith wave component. μ_i is measured positive in the counterclockwise direction looking down, which is in accordance with the right-hand rule.

Subsequently, we consider that the wave groups consisting of two incident linear waves interacts with a vertical wall. For the case that the wave groups consisting of two regular waves are fully reflected, the vertical wall behaves like a mirror. Therefore, the total wave field after the interaction of wave groups with a vertical wall is equivalent to that of wave groups composed of two incident regular waves and two mirrored regular waves, as shown in Fig. 2. This means that for the reflection problem, there are four regular wave components that interact with one another. And the incident and mirrored wave components satisfy the following equation,

$$\omega_i = \omega_i', \ \left|\overrightarrow{k}_i\right| = \left|\overrightarrow{k}_i'\right|, \ \mu_i + \mu_i' = \pi \tag{16}$$

where, ω_i', $\overrightarrow{k}_i'$ and μ_i' $(i = 1, 2)$ are, respectively, the circular frequency, wave number and propagating direction for the mirrored (or reflected) wave components.

The phase functions for the incident and mirrored wave components are as follows,

$$\left.\begin{aligned} \psi_i &= \overrightarrow{k}_i \cdot \overrightarrow{X} - \omega_i t + \varepsilon_i \\ \psi_i' &= \overrightarrow{k}_i' \cdot \left(\overrightarrow{X} - 2\overrightarrow{X}_1\right) - \omega_i t + \varepsilon_i \end{aligned}\right\} \tag{17}$$

where, $\overrightarrow{X}_1 = (x_1, 0)$.

As a result, the results of surface elevation derived by Sharma and Dean (1981) or Dalzell (1999) can be extended to the total wave field, η^T, after reflection by a vertical wall,

$$\begin{aligned} \eta^T = &\sum_{i=1}^{2}\left(a_i \cos\psi_i + a_i' \cos\psi_i'\right) + a_1 a_1' B_{11}^{+\prime} \cos\left(\psi_1 + \psi_1'\right) \\ &+ a_2 a_2' B_{22}^{+\prime} \cos\left(\psi_2 + \psi_2'\right) + a_1 a_2 B_{12}^{+} \cos\left(\psi_1 + \psi_2\right) \\ &+ a_1' a_2' B_{12}^{+''} \cos\left(\psi_1' + \psi_2'\right) + a_1 a_2' B_{12}^{+\prime} \cos\left(\psi_1 + \psi_2'\right) \\ &+ a_1' a_2 B_{21}^{+\prime} \cos\left(\psi_1' + \psi_2\right) + a_1 a_1' B_{11}^{-\prime} \cos\left(\psi_1 - \psi_1'\right) \\ &+ a_2 a_2' B_{22}^{-\prime} \cos\left(\psi_2 - \psi_2'\right) + a_1 a_2 B_{12}^{-} \cos\left(\psi_1 - \psi_2\right) \\ &+ a_1' a_2' B_{12}^{-''} \cos\left(\psi_1' - \psi_2'\right) + a_1 a_2' B_{12}^{-\prime} \cos\left(\psi_1 - \psi_2'\right) \\ &+ a_1' a_2 B_{21}^{-\prime} \cos\left(\psi_1' - \psi_2\right) \\ &+ \sum_{i=1}^{2}\left\{\frac{a_i^2\left|\overrightarrow{k}_i\right|}{4\tanh\left(\left|\overrightarrow{k}_i\right| h\right)}\left(2 + \frac{3}{\sinh^2\left(\left|\overrightarrow{k}_i\right| h\right)}\right)\cos(2\psi_i)\right. \\ &\left. + \frac{a_i'^2\left|\overrightarrow{k}_i'\right|}{4\tanh\left(\left|\overrightarrow{k}_i'\right| h\right)}\left(2 + \frac{3}{\sinh^2\left(\left|\overrightarrow{k}_i'\right| h\right)}\right)\cos\left(2\psi_i'\right)\right\} \\ &- \sum_{i=1}^{2}\left(\frac{a_i^2\left|\overrightarrow{k}_i\right|}{2\sinh\left(2\left|\overrightarrow{k}_i\right| h\right)} + \frac{a_i'^2\left|\overrightarrow{k}_i'\right|}{2\sinh\left(2\left|\overrightarrow{k}_i'\right| h\right)}\right) \end{aligned} \tag{18}$$

where, $B_{ij}^{+\prime}$ and $B_{ij}^{-\prime} (i = 1, 2; j = 1, 2)$ indicate the interaction term for the ith incident wave component and jth mirrored wave component. B_{12}^{+} and B_{12}^{-} are the interaction term for the two incident wave components. $B_{12}^{+''}$ and $B_{12}^{-''}$ are the interaction term for two mirrored (or reflected) wave components. These interaction terms are calculated by substituting the

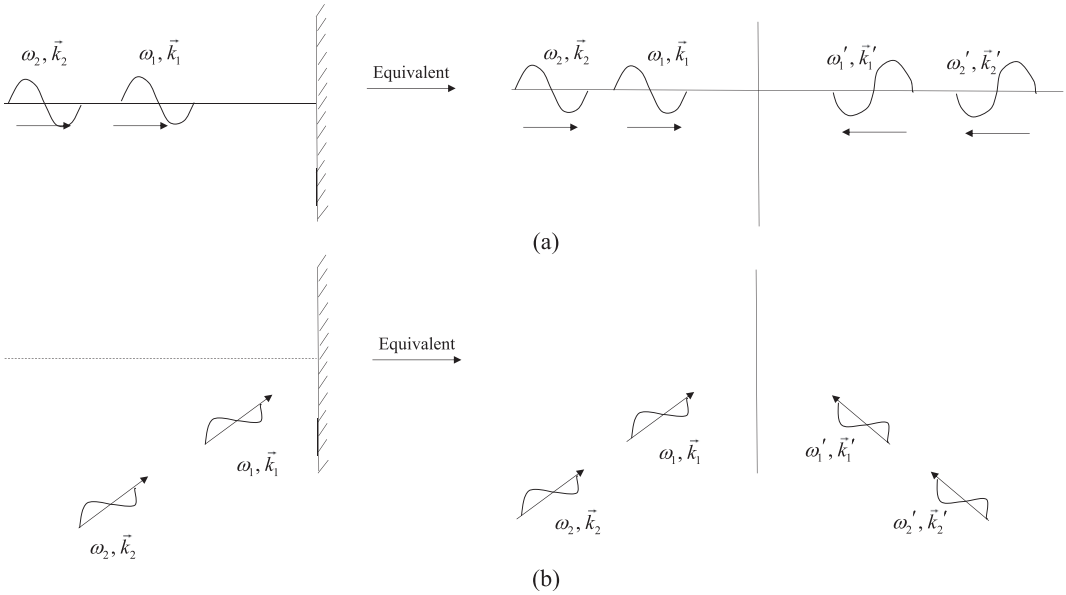

Fig. 2. Equivalence of the wave field between wave groups of two regular waves reflected by a vertical wall and wave groups consisting of two incident and two mirrored regular waves: (a) front view; (b) top view.

Please cite this article in press as: Sun, Y., Zhang, X., A second order analytical solution of focused wave group interacting with a vertical wall, International Journal of Naval Architecture and Ocean Engineering (2016), http://dx.doi.org/10.1016/j.ijnaoe.2016.09.002

corresponding values of frequency, wave number and angle of incidence into Eqs. (12) and (13).

If we denote $_3$ and $_4$ as the mirrored wave component corresponding to the first and second incident wave component, respectively, i.e. $\omega_3 = \omega_1'$, $\omega_4 = \omega_2'$, $\vec{k}_3 = \vec{k}_1'$, $\vec{k}_4 = \vec{k}_2$, then we can re-express Eq. (18) as follows,

$$\begin{aligned}\eta^T = &\sum_{i=1}^{4} a_i \cos\psi_i + \sum_{i=1}^{3}\sum_{j=i+1}^{4}\Big(a_i a_j B_{ij}^{+}\cos(\psi_i+\psi_j) \\ &+ a_i a_j B_{ij}^{-}\cos(\psi_i-\psi_j)\Big) \\ &+ \sum_{i=1}^{4}\left\{\frac{a_i^2|\vec{k}_i|}{4\tanh(|\vec{k}_i|h)}\left(2+\frac{3}{\sinh^2(|\vec{k}_i|h)}\right)\cos(2\psi_i)\right\} \\ &- \sum_{i=1}^{4}\frac{a_i^2|\vec{k}_i|}{2\sinh(2|\vec{k}_i|h)}\end{aligned} \tag{19}$$

Similarly, we get the velocity potential, ϕ^T, of total wave field as follows,

$$\begin{aligned}\phi^T = &\sum_{i=1}^{4}\left\{a_i\frac{g}{\omega_i}\frac{\cosh\{|\vec{k}_i|(z+h)\}}{\cosh(|\vec{k}_i|h)}\sin\psi_i\right\} \\ &+ \sum_{i=1}^{4}\left\{a_i^2\frac{3}{8}\omega_i\frac{\cosh\{2|\vec{k}_i|(z+h)\}}{\sinh^4(|\vec{k}_i|h)}\sin(2\psi_i)\right\} + \sum_{i=1}^{3} \\ &\times\sum_{j=i+1}^{4}\left\{a_i a_j A_{ij}^{+}\frac{\cosh\{|\vec{k}_i+\vec{k}_j|(z+h)\}}{\cosh(|\vec{k}_i+\vec{k}_j|h)}\sin(\psi_i+\psi_j)\right. \\ &\left.+ a_i a_j A_{ij}^{-}\frac{\cosh\{|\vec{k}_i-\vec{k}_j|(z+h)\}}{\cosh(|\vec{k}_i-\vec{k}_j|h)}\sin(\psi_i-\psi_j)\right\}\end{aligned} \tag{20}$$

Next step, we extend the total wave field composed of two incident regular wave components and two mirrored wave components, to the ones consisting of N incident regular wave components and N corresponding mirrored wave components. First, the symbol i ($i = 1, 2,\ldots, N$) represents the ith incident wave component and the symbol $N + i$ indicates the ith mirrored wave component corresponding to the ith incident wave component. Then we get the surface wave elevation and velocity potential of the total wave field as follows,

$$\begin{aligned}\eta^T = &\sum_{i=1}^{2N} a_i \cos\psi_i + \sum_{i=1}^{2N-1}\sum_{j=i+1}^{2N}\Big\{a_i a_j B_{ij}^{+}\cos(\psi_i+\psi_j) \\ &+ a_i a_j B_{ij}^{-}\cos(\psi_i-\psi_j)\Big\} \\ &+ \sum_{i=1}^{2N}\left\{\frac{a_i^2|\vec{k}_i|}{4\tanh(|\vec{k}_i|h)}\left(2+\frac{3}{\sinh^2(|\vec{k}_i|h)}\right)\cos(2\psi_i)\right\} \\ &- \sum_{i=1}^{2N}\frac{a_i^2|\vec{k}_i|}{2\sinh(2|\vec{k}_i|h)}\end{aligned} \tag{21}$$

$$\begin{aligned}\phi^T = &\sum_{i=1}^{2N}\left\{a_i\frac{g}{\omega_i}\frac{\cosh\{|\vec{k}_i|(z+h)\}}{\cosh(|\vec{k}_i|h)}\sin\psi_i\right\} \\ &+ \sum_{i=1}^{2N}\left\{a_i^2\frac{3}{8}\omega_i\frac{\cosh\{2|\vec{k}_i|(z+h)\}}{\sinh^4(|\vec{k}_i|h)}\sin(2\psi_i)\right\} + \sum_{i=1}^{2N-1} \\ &\times\sum_{j=i+1}^{2N}\left\{a_i a_j A_{ij}^{+}\frac{\cosh\{|\vec{k}_i+\vec{k}_j|(z+h)\}}{\cosh(|\vec{k}_i+\vec{k}_j|h)}\sin(\psi_i+\psi_j)\right. \\ &\left.+ a_i a_j A_{ij}^{-}\frac{\cosh\{|\vec{k}_i-\vec{k}_j|(z+h)\}}{\cosh(|\vec{k}_i-\vec{k}_j|h)}\sin(\psi_i-\psi_j)\right\}\end{aligned} \tag{22}$$

where,

$$\omega_{N+i} = \omega_i, |\vec{k}_{N+i}| = |\vec{k}_i|, \mu_{N+i} + \mu_i = \pi \tag{23}$$

and

$$\left.\begin{aligned}\psi_i &= \vec{k}_i\cdot\vec{X} - \omega_i t + \varepsilon_i \\ \psi_{N+i} &= \vec{k}_{N+i}\cdot(\vec{X} - 2\vec{X}_1) - \omega_{N+i}t + \varepsilon_i\end{aligned}\right\} \tag{24}$$

Specifically, we consider focused wave groups based on NewWave theory (Tromans et al., 1991) with focal position $\vec{x}_0$ and focal time t_0. The amplitude of each wave component is

$$a_i = A\frac{S_i(f)\Delta f}{\sum_{j=1}^{N} S_j(f)\Delta f} \tag{25}$$

where $S(f)$ is the spectral density for a given frequency f, Δf is the frequency step calculated as $\Delta f = (f_u - f_l)/(N-1)$ with f_u and f_l being, respectively, the upper and lower limit of a given frequency bandwidth. A is the linear amplitude of peak crest of focused wave groups.

In our simulation, the Joint North Sea Wave Project (JONSWAP) spectrum (Hasselmann et al., 1973) is adopted, the spectral density of which is described as follows,

$$S(f) = \alpha H_s^2 T_p^{-4} f^{-5}\exp\left[-1.25(T_p f)^{-4}\right]\chi^{\exp\left[-(T_p f-1)^2/(2\sigma^2)\right]} \tag{26}$$

where H_s is the significant wave height, T_p is the peak period of the JONWAP spectrum and χ is the peak lifting factor. The power density at the peak frequency is larger for larger value of the peak lifting factor (see Fig. 17). σ is the peak shape parameter, the value of which is defined as,

$$\sigma = \begin{cases}0.09 & for\ f \geq f_p \\ 0.07 & for\ f < f_p\end{cases} \tag{27}$$

where $f_p = 1/T_p$ is the peak frequency. α is a coefficient that is related to the peak lifting factor χ as follows,

$$\alpha = \frac{0.0624}{0.230 + 0.0336\chi - 0.185/(1.9+\chi)} \tag{28}$$

Please cite this article in press as: Sun, Y., Zhang, X., A second order analytical solution of focused wave group interacting with a vertical wall, International Journal of Naval Architecture and Ocean Engineering (2016), http://dx.doi.org/10.1016/j.ijnaoe.2016.09.002

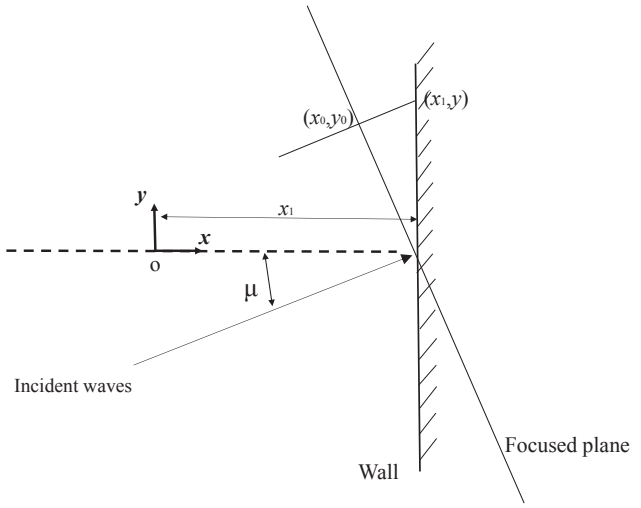

Fig. 3. Definition of focused positions for obliquely-incident focused wave groups interacting with a vertical wall.

And by setting the value of random phase $\varepsilon_i = -\vec{k}_i \cdot \vec{x}_0 + \omega_i t_0$ ($i = 1, 2, \ldots, N$), the phase function shown in Eq. (24) is obtained as follows,

$$\begin{aligned} \psi_i &= \vec{k}_i \cdot \left(\vec{X} - \vec{x}_0\right) - \omega_i (t - t_0) \\ \psi_{N+i} &= \vec{k}_{N+i} \cdot \left(\vec{X} - 2\vec{X}_1\right) - \vec{k}_i \cdot \vec{x}_0 - \omega_i (t - t_0) \end{aligned} \tag{29}$$

Combining Eqs. (21)–(29), we get the surface elevation and velocity potential of NewWave type focused wave groups interacting with a semi-infinite vertical wall.

After obtaining the expressions of velocity potential and surface elevation of nonlinear focused wave groups after reflection of a vertical wall, the pressure along the vertical wall can be calculated. Then the force, F, exerted by focused wave groups on the vertical wall, per unit of distance in the y direction, is obtained by integrating the pressure along the vertical wall. The pressure equation (also called Bernoulli equation) is given as follows,

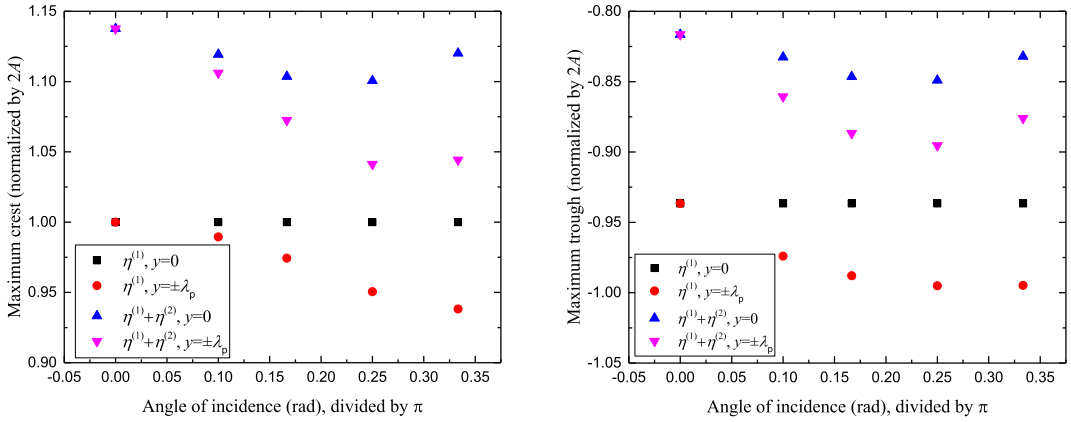

Fig. 4. Variation of the maximum crest and trough at the vertical wall with the angle of incidence of focused wave groups: (a) the normalized maximum crest and (b) the normalized maximum trough.

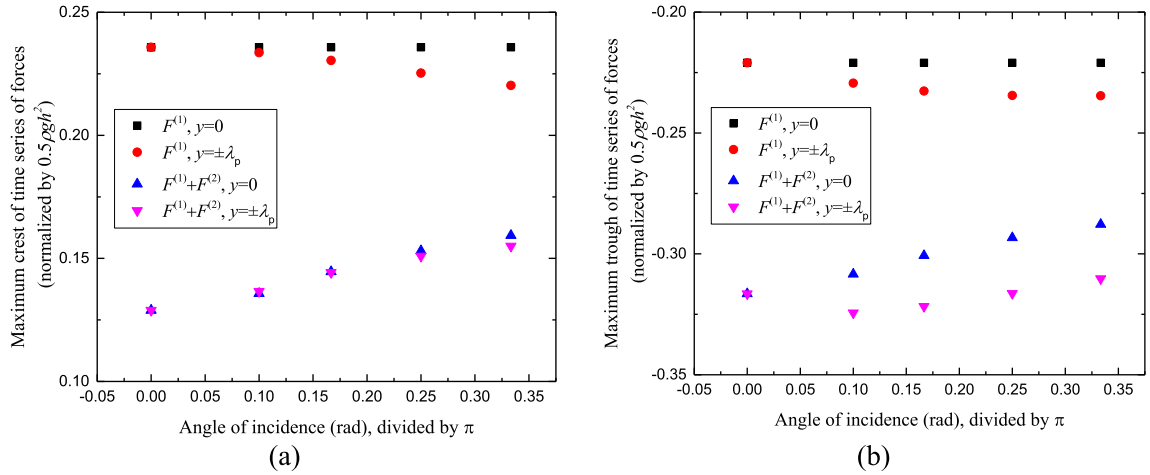

Fig. 5. Variation of the maximum crest and trough of time series of wave forces at the vertical wall with the angle of incidence of focused wave groups: (a): the normalized maximum crest and (b): the normalized maximum trough.

Please cite this article in press as: Sun, Y., Zhang, X., A second order analytical solution of focused wave group interacting with a vertical wall, International Journal of Naval Architecture and Ocean Engineering (2016), http://dx.doi.org/10.1016/j.ijnaoe.2016.09.002

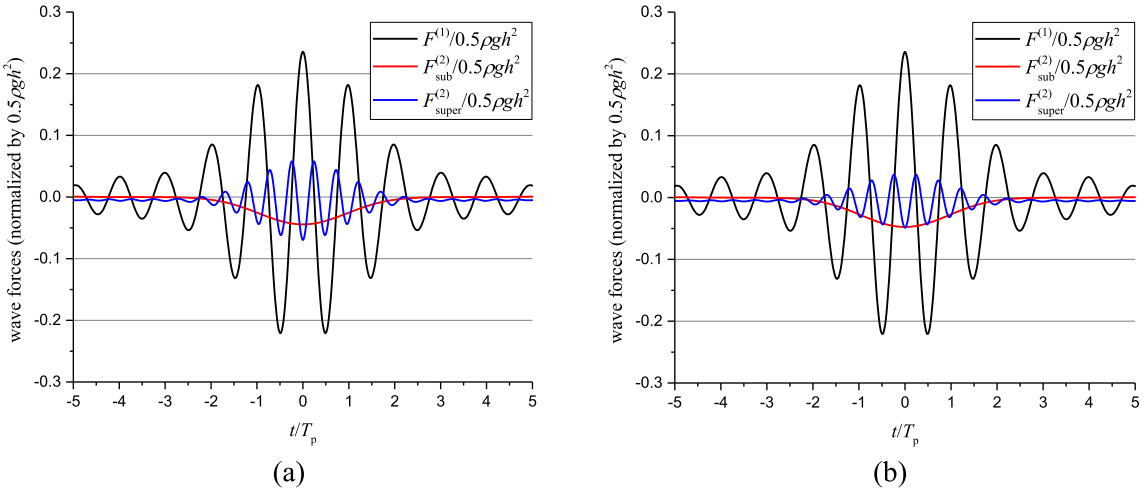

Fig. 6. Time series of wave forces on the vertical wall for different angles of incidence at $y = 0$, (a) $\mu = 0$; (b) $\mu = \pi/6$. $F^{(2)}_{sub}$ and $F^{(2)}_{super}$ are, respectively, the sub- and super-harmonics of the second order force terms.

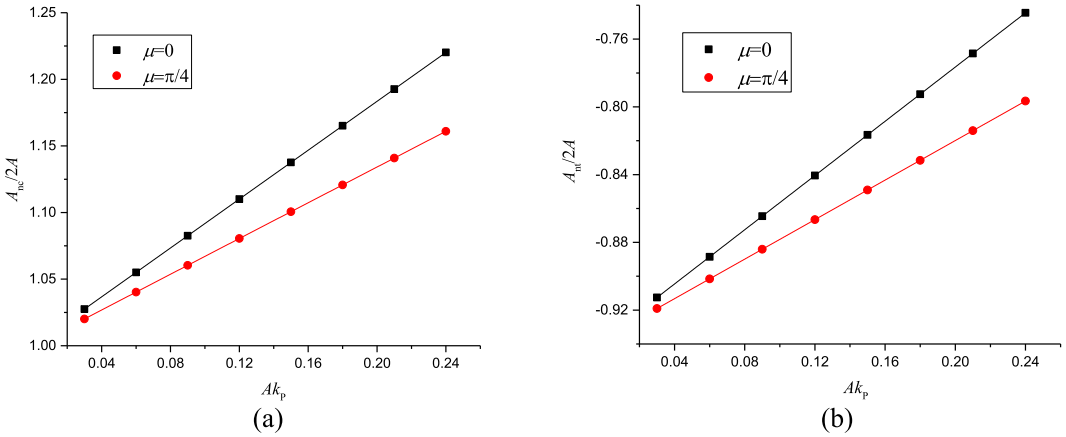

Fig. 7. Variation of the maximum nonlinear crest or trough with wave steepness of incident focused wave groups, (a) the maximum crest (A_{nc}) and (b) the maximum trough (A_{nt}).

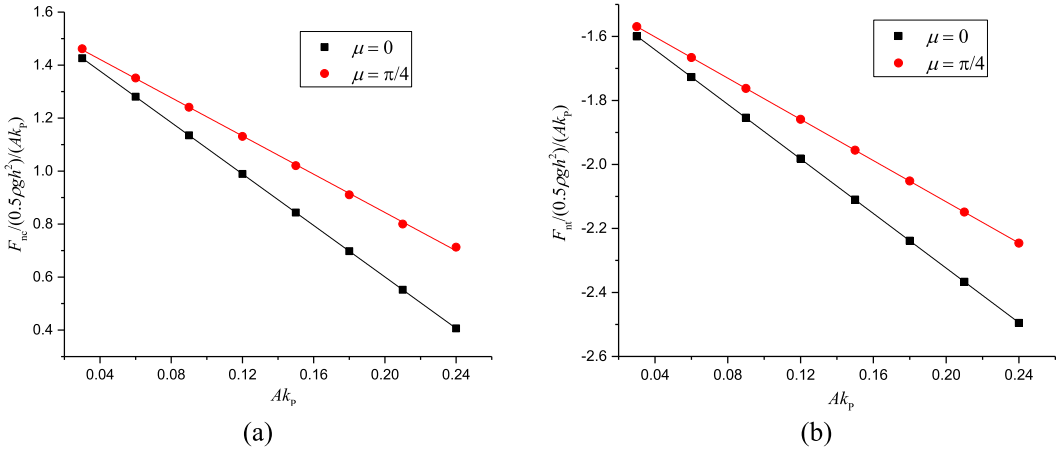

Fig. 8. Variation of the maximum nonlinear crest or trough of wave force time series with wave steepness of incident focused wave groups, (a) the maximum crest (F_{nc}) and (b) the maximum trough (F_{nt}).

Please cite this article in press as: Sun, Y., Zhang, X., A second order analytical solution of focused wave group interacting with a vertical wall, International Journal of Naval Architecture and Ocean Engineering (2016), http://dx.doi.org/10.1016/j.ijnaoe.2016.09.002

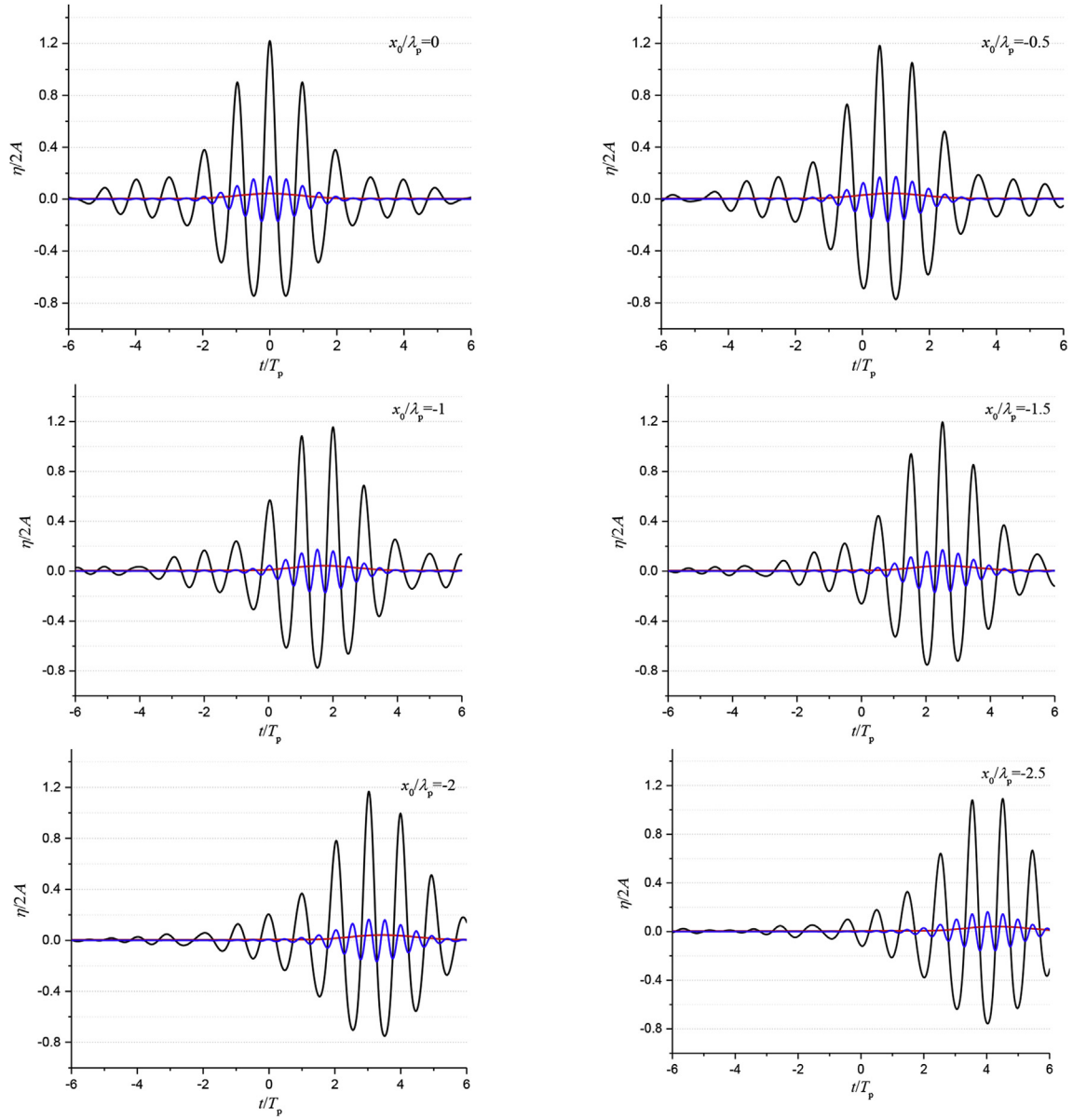

Fig. 9. The nonlinear focused wave group profile and its second order component in time domain at the vertical wall (black line-the nonlinear wave elevation; red line-the second order sub-harmonics and blue line-the second order super-harmonics). A vertical wall is located at $x = 0$ and the nonlinear wave group focuses at $t = 0$ and $x = x_0$. The time is normalized by peak period T_p and the wave elevation is normalized by twice of the peak wave crest, $2A$.

$$\frac{P}{\rho} = -gz - \frac{\partial\phi}{\partial t} - \frac{1}{2}\left[\left(\frac{\partial\phi}{\partial x}\right)^2 + \left(\frac{\partial\phi}{\partial y}\right)^2 + \left(\frac{\partial\phi}{\partial z}\right)^2\right] \tag{30}$$

And the wave force is given as

$$F = \int_{-h}^{\eta} P(x_1, y, z, t)dz \tag{31}$$

If we denote $^{(1)}$ and $^{(2)}$ as the first and second order term in terms of a small perturbation parameter (such as the wave steepness), then the surface elevation and velocity potential of the total wave field as shown in Eq. (21) and (22) can be re-expressed as

$$\eta^T = \eta^{(1)} + \eta^{(2)} \tag{32}$$

$$\phi^T = \phi^{(1)} + \phi^{(2)} \tag{33}$$

Similarly, the pressure can be expanded, correct to second order, as

$$P = P^{(0)} + P^{(1)} + P^{(2)} \tag{34}$$

with

$$P^{(0)} = -\rho gz \tag{35}$$

Please cite this article in press as: Sun, Y., Zhang, X., A second order analytical solution of focused wave group interacting with a vertical wall, International Journal of Naval Architecture and Ocean Engineering (2016), http://dx.doi.org/10.1016/j.ijnaoe.2016.09.002

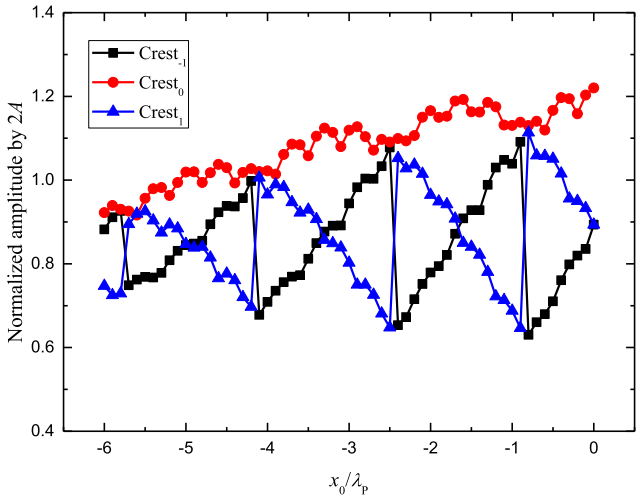

Fig. 10. The characteristics of the crest amplitude for different focal positions, x_0. Crest_0, Crest_{-1} and Crest_{+1} represent, respectively, the maximum crest and the crest ahead of and after the maximum crest.

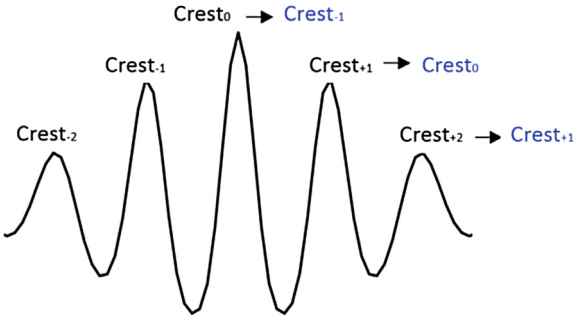

Fig. 11. Transformation of the three largest wave crests.

$$P^{(1)} = -\rho \frac{\partial \phi^{(1)}}{\partial t} \tag{36}$$

$$P^{(2)} = -\rho \frac{\partial \phi^{(2)}}{\partial t} - \frac{1}{2}\rho \left[\left(\frac{\partial \phi^{(1)}}{\partial x} \right)^2 + \left(\frac{\partial \phi^{(1)}}{\partial y} \right)^2 + \left(\frac{\partial \phi^{(1)}}{\partial z} \right)^2 \right] \tag{37}$$

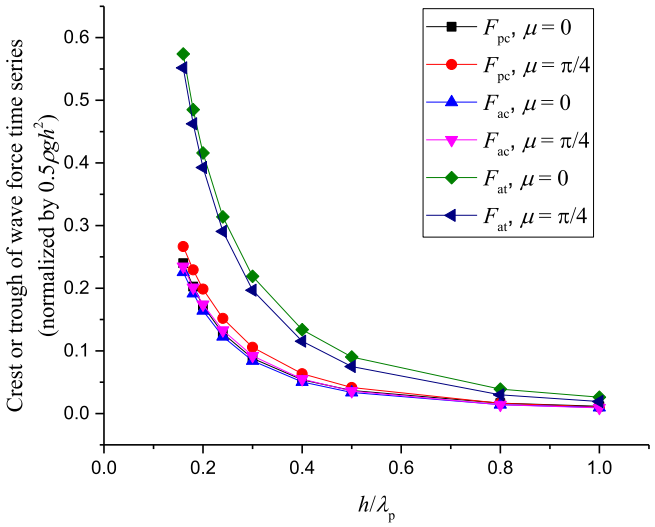

Fig. 13. Effects of water depth on wave force time series. F_{pc}, F_{ac} and F_{at} represent, respectively, the peak crest, adjacent crest and adjacent trough of wave force time series.

Then the wave force along the vertical wall can also be divided into the hydrostatic term, the first and second order term, i.e.

$$F = F^{(0)} + F^{(1)} + F^{(2)} \tag{38}$$

The calculation of the wave force is shown in Appendix A.

4. Results and discussion

In this section, a detailed investigation is made on the interaction between focused wave groups and a vertical wall with effects of different parameters considered. Particular attention will be put to the surface elevation along the vertical wall and the impact force on the vertical wall. The former one may provide a preliminary insight into wave run up and overtopping events, and the latter one is of great significance in structural design of the seawall.

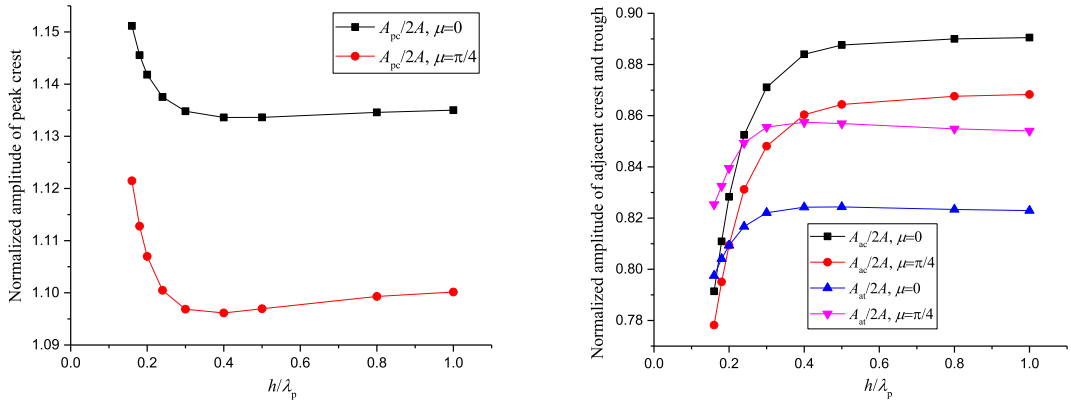

Fig. 12. Effects of water depth on the surface elevation of nonlinear focused wave groups interacting with a vertical wall, (a) the peak crest; (b) the adjacent crest and trough. A_{pc}, A_{ac} and A_{at} represent, respectively, the peak crest, adjacent crest and adjacent trough of the surface elevation.

Please cite this article in press as: Sun, Y., Zhang, X., A second order analytical solution of focused wave group interacting with a vertical wall, International Journal of Naval Architecture and Ocean Engineering (2016), http://dx.doi.org/10.1016/j.ijnaoe.2016.09.002

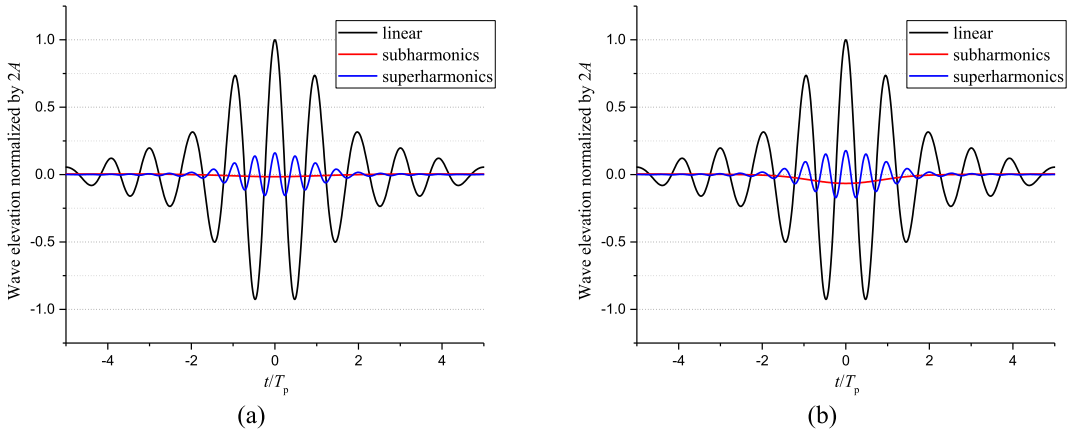

Fig. 14. Surface elevation of focused wave groups at the vertical wall. The water depth is $0.18\lambda_p$, (a) the case for $\mu = 0$ and (b) the case for $\mu = \pi/4$.

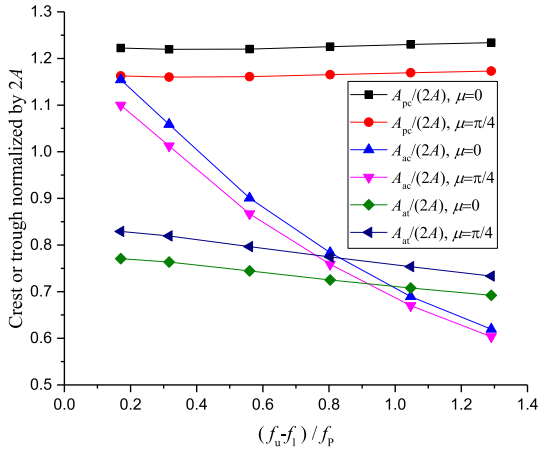

Fig. 15. The effects of frequency bandwidth on the focused wave groups that interact with the vertical wall.

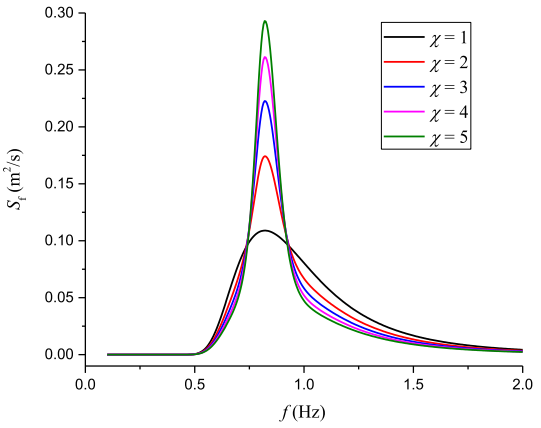

Fig. 17. Spectral density for different peak lifting factors (JONSWAP spectrum): $H_s = 1$ m.

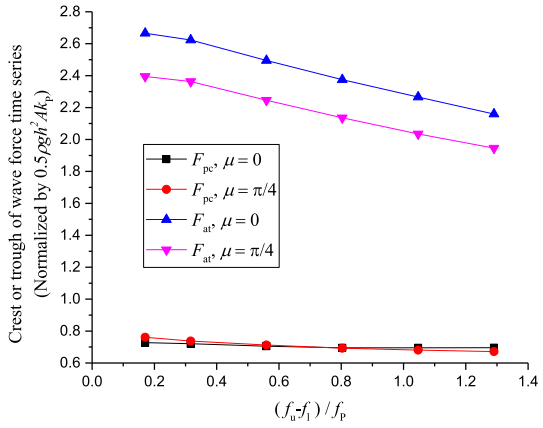

Fig. 16. The effects of frequency bandwidth on the wave forces exerted on the vertical wall.

4.1. The effects of the angle of incidence

For normally incident focused wave groups, the focused plane (or the peak crest line) is parallel to the vertical wall. However, for obliquely-incident focused wave groups, there is an inclination angle between the focused plane and the vertical wall. The definition of focused positions is shown in Fig. 3. The focused position is related to the point on the vertical wall as follows,

$$\left.\begin{aligned} x_0 &= x_1 - y\cos\mu\sin\mu \\ y_0 &= y\cos^2\mu \end{aligned}\right\} \tag{39}$$

Then we will investigate the effects of the angle of incidence of focused wave groups on the surface elevation, as well as wave forces on the vertical wall. Parameters of focused wave groups are summarized in Table 1. For normally-incident focused wave groups ($\mu = 0$), the focused position is set at the vertical wall. And for obliquely-incident focused wave groups, without loss of generality, the intersection between the vertical wall and the focused plane is on the plane $y = 0$.

The effects of angles of incidence of focused wave groups on surface elevation are given in Fig. 4. It is clear that the linear theory (the first order term) underestimates the crest and overestimates the trough. At $y = 0$, although the linear maximum crest stays unchanged for different angles of incidence, the nonlinear maximum crest decreases slightly with the increase of the angle of incidence. However, there is a slight rise for the angle changing from $\pi/4$ to $\pi/3$. This trend

Please cite this article in press as: Sun, Y., Zhang, X., A second order analytical solution of focused wave group interacting with a vertical wall, International Journal of Naval Architecture and Ocean Engineering (2016), http://dx.doi.org/10.1016/j.ijnaoe.2016.09.002

Table 1
Parameters of focused wave groups used for considering effects of angles of incidence.

Frequency brandwidth, f_l–f_u (Hz)	Number of wave components, N	Water depth, h, (m)	Peak lifting factor, χ	Peak wave number, k_p (m^{-1})	Peak crest, A (m)	Wave steepness, Ak_p
0.6–1.06	29	0.5	3.3	3	0.05	0.15

(in accordance with the maximum crest of second order terms) is caused by the second order nonlinear effects of wave–wave and wave structure interaction. The nonlinear maximum crest at $y = \pm\lambda_P$ is smaller than that at $y = 0$, the difference of which becomes larger for larger angle of incidence. A possible explanation of this phenomenon is that the distance between the point at the vertical wall and the corresponding focused position is larger for larger value of angle of incidence. In contrast to crest, the maximum trough of surface elevation first increases and then reduces with the angle of incidence. The trough at $y = \pm\lambda_P$ (λ_P is the peak wave length corresponding to the peak period) is deeper than that at $y = 0$.

Fig. 5 shows the first and second order terms of wave forces exerted on the vertical wall for different angles of incidence. The linear theory (the first order term) overestimates the crest and underestimates the trough of the time series of hydrodynamic forces on the vertical wall. The nonlinear maximum crest rises with the angle of incidence while the trough shows an opposite trend. This is due to the second order effects. For the purpose of illustration, the time series of wave forces (including the first order term and the second order sub- and super-harmonics) for angles of incidence being 0 and $\pi/6$ are given in Fig. 6. The sub-harmonics is almost the same for two angles of incidence. However, the super-harmonics has a larger amplitude of trough at $\mu = 0$ than at $\mu = \pi/6$. Thus the nonlinear wave force at $\mu = 0$ has a smaller crest and a larger trough than that at $\mu = \pi/6$. Finally, it is interesting to note that for obliquely-incident focused wave groups, the maximum crest of wave force is less sensitive to the position at the vertical wall than the maximum trough.

4.2. The effects of wave steepness of incident focused wave groups

In this section, a detailed investigation is put on the effects of wave steepness on the largest crest and trough of wave groups, as well as wave forces. The parameters of focused wave groups with different wave steepness are given in Table 2. Two angles of incidence are chosen: $\mu = 0$ and $\mu = \pi/4$. The position is at y = 0 of the vertical wall. It can be seen from Fig. 7 that both the normalized largest crest and trough vary at a uniform rate with wave steepness, which is consistent with the second order assumption. By fitting the data using least square method, we get two equations, i.e. Eqs. (40) and (41). The rate of variation of the largest crest (0.92 for $\mu = 0$) is larger than that of the largest trough (0.80 for $\mu = 0$), which indicates that the crest is more sensitive to the nonlinear effects than the trough. By comparing Eqs. (40) and (41), we find that the increase of angles of incidence causes both the largest crest and trough to be less sensitive to the second order effects.

As can be seen form Fig. 8, the normalized maximum crest or trough of wave force time series also varies at a uniform rate with wave steepness, but reduces as the wave steepness increases. The crest or trough is more influenced by the second order nonlinear effects at $\mu = 0$ than at $\mu = \pi/4$. Fitting expressions by the least square method are given in Eqs. (42) and (43).

$$\mu = 0: \begin{cases} \dfrac{A_{nc}}{2A} = 1 + 0.92Ak_P \\ \dfrac{A_{nt}}{2A} = -0.94 + 0.80Ak_P \end{cases} \tag{40}$$

$$\mu = \frac{\pi}{4}: \begin{cases} \dfrac{A_{nc}}{2A} = 1 + 0.67Ak_P \\ \dfrac{A_{nt}}{2A} = -0.94 + 0.58Ak_P \end{cases} \tag{41}$$

$$\mu = 0: \begin{cases} \dfrac{F_{nc}}{(0.5\rho g h^2)(Ak_P)} = 1.572 - 4.856Ak_P \\ \dfrac{F_{nt}}{(0.5\rho g h^2)(Ak_P)} = -1.471 - 4.264Ak_P \end{cases} \tag{42}$$

$$\mu = \frac{\pi}{4}: \begin{cases} \dfrac{F_{nc}}{(0.5\rho g h^2)(Ak_P)} = 1.566 - 3.611Ak_P \\ \dfrac{F_{nt}}{(0.5\rho g h^2)(Ak_P)} = -1.473 - 3.220Ak_P \end{cases} \tag{43}$$

4.3. The effects of focal positions on the evolution of focused wave groups interacting with a vertical wall

In this section, the effects of focal positions on the evolution of focused wave groups that interact with a vertical wall

Table 2
Parameters of focused wave groups of different wave steepness.

Frequency brandwidth, f_l–f_u (Hz)	Number of wave components, N	Water depth, h, (m)	Peak lifting factor, χ	Peak wavelength, k_p (m)	Peak crest, A (m)	Wave steepness, Ak_p
0.6–1.06	29	0.5	3.3	3	0.01–0.08	0.03–0.24

Please cite this article in press as: Sun, Y., Zhang, X., A second order analytical solution of focused wave group interacting with a vertical wall, International Journal of Naval Architecture and Ocean Engineering (2016), http://dx.doi.org/10.1016/j.ijnaoe.2016.09.002

Table 3
Parameters of focused wave groups used for considering effects of focal positions.

Frequency brandwidth, f_l–f_u (Hz)	Number of wave components, N	Water depth, h, (m)	Peak lifting factor, χ	Peak wavelength, k_p (m)	Peak crest, A (m)	Wave steepness, Ak_p
0.6–1.06	29	0.5	3.3	3	0.08	0.24

are investigated. Only normally-incident waves are considered. The parameters of focused wave groups are given in Table 3. Fig. 9 shows the wave elevation (including nonlinear elevation and sub- and super-harmonics of the second order terms) at the vertical wall for different focal positions. It can be found that for the case $x_0/\lambda_P = 0$, i.e. wave groups focussing at the vertical wall, the main features of focused wave groups are maintained. The wave elevation reaches its maximum at the focal time $t_0 = 0$ and presents symmetric shapes before and after $t_0 = 0$. When the focal position of wave groups is set at any point in front of the wall, the wave elevation at the vertical wall is no longer symmetric around the maximum crest. The adjacent crest ahead of the maximum one may be larger or smaller than that after the maximum one, which depends on the focal positions. As indicated by Fig. 11, Crest_0 and $\text{Crest}_{\pm i}$ ($i = 1, 2,\ldots$) represent, respectively the largest crest and adjacent crests.

A detailed investigation of variation of the maximum crest and its adjacent crests with respect to focal positions is shown in Fig. 10. With the increase of the distance of focal positions from the vertical wall, the maximum crest, although fluctuating, gradually decreases. The normalized crest amplitude at the vertical wall is 1.22 for $x_0/\lambda_P = 0$. However, this value decreases to be 0.92 for $x_0/\lambda_P = -6$. It can also be found from Fig. 10 that the variation of focal positions has great effects on adjacent crests. With focal positions deviating from the vertical wall, the adjacent crest at the left side starts to decrease and the right one increases. Then at $x_0/\lambda_P = -0.8$, the first transformation of three largest crests occurs (see Fig. 11), i.e. the previous three crests including Crest_0, Crest_{+1} and Crest_{+2} are, respectively, transformed into the current three wave crests – Crest_{-1}, Crest_0 and Crest_{+1}. As a result, the adjacent crest at the left side of the maximum crest becomes larger than that at the right side. With the distance of focal positions from the vertical wall continuing to increase, the amplitude of Crest_{-1} decreases and Crest_{+1} increases. Then two adjacent crests at the opposite sides of the maximum crest are almost equal to each other at $x_0/\lambda_P = -1.6$, followed by which Crest_{-1} continues to decrease and becomes smaller than Crest_{+1}. At $x_0/\lambda_P = -2.4$, there is a new transformation, after which similar variation of Crest_{-1} and Crest_{+1} occurs as before. Summarily, the transformation of the largest three crests (shown in Fig. 11) occurs at some specific positions in front of the vertical wall, which satisfies

$$x_0/\lambda_p = -(2k+1) \times 0.8, k = 0, 1, 2, \ldots \quad (44)$$

And in one transformation circle, the amplitude of Crest_{-1} can be larger or smaller than that of Crest_{+1}, depending on the following critical focused position,

$$x_0/\lambda_p = -2k \times 0.8, k = 0, 1, 2, \ldots \quad (45)$$

If the distance of focal positions from the vertical wall is smaller than that of the critical point, Crest_{-1} is larger than Crest_{+1}. Otherwise, the amplitude of the former is smaller than that of the latter. The difference of the amplitude between two adjacent crests at both sides of the maximum crest becomes smaller at the critical point as the focal position is far away from the vertical wall.

4.4. The effects of water depth

The effects of water depth on the interaction between focused wave groups and a vertical wall are studied in this section. Parameters of focused wave groups used here are given in Table 4. Results of surface elevation and wave force time series are shown in Figs. 12 and 13, respectively. It should be noted that the second order theory cannot be applied to extremely shallow water depth as unphysical "bumps" will be formed in the wave trough due to the second order terms. So the smallest water depth considered here (no obvious bumps in the wave trough) is $h = 0.16\lambda_P$.

It can be seen From Fig. 12 that the variation of surface profile with respect to water depth for $\mu = 0$ is similar to that for $\mu = \pi/4$. For deep water conditions ($h/\lambda_P > 0.5$), the surface elevation profile keeps almost unchanged for different water depth. When the normalized water depth is less than 0.5 (finite water depth), the amplitude of peak crest increases with the decrease of water depth. However, the adjacent crest decreases for shallower water depth. This indicates that shallow water effects will lead to more energy transferred from surrounding waves to the central wave. For wave trough, there is a slight increase for normalized water depth reducing from 1.0 to 0.3, followed by which an increase occurs for shallower water depth (from 0.3 to 0.16). An illustration of wave profiles for $h = 0.18\lambda_P$ (including both linear term and sub- and super-harmonics of the second order term) is given in Fig. 14.

As shown in Fig. 13, with the decrease of water depth, the peak crest, adjacent crest and adjacent trough of wave force

Table 4
Parameters of focused wave groups of different water depth.

Frequency brandwidth, f_l–f_u (Hz)	Number of wave components, N	Water depth, h, (m)	Peak lifting factor, χ	Peak wavelength, k_p (m)	Peak crest, A (m)	Wave steepness, Ak_p
0.6–1.06	29	0.34–2.1	3.3	3	0.05	0.15

Please cite this article in press as: Sun, Y., Zhang, X., A second order analytical solution of focused wave group interacting with a vertical wall, International Journal of Naval Architecture and Ocean Engineering (2016), http://dx.doi.org/10.1016/j.ijnaoe.2016.09.002

time series increase. There is little difference between the peak crest and adjacent crest. The effect of angles of incidence on peak crest, adjacent crest and adjacent trough is relatively noticeable in intermediate water depth.

4.5. The effects of frequency bandwidth on the evolution of focused wave groups interacting with the vertical wall

In this section, effects of frequency bandwidth (i.e. f_u-f_l) on the interaction between focused wave groups and a vertical wall are investigated. The parameters for wave groups with different frequency bandwidth are shown in Table 5. The peak frequency of JONSWAP spectrum is kept unchanged. The frequency interval, i.e. $\Delta f=(f_u-f_l)/N$, is nearly identical for five cases. The focal position of wave groups is set at the vertical wall for all cases.

For focused wave groups interacting with a vertical wall, the peak crest of wave elevation varies little with the frequency bandwidth (Fig. 15). However, both the adjacent crest and the trough reduce with the increase of frequency bandwidths. And the former decreases at a higher rate than the latter (the decreasing rate is almost uniform). Besides, it seems that the angle of incidence has no significant effects on the decreasing rate.

Similarly shown in Fig. 16, the crest of wave force time series is not much influenced by the frequency bandwidth while the trough reduces at a nearly uniform rate with the increase of frequency bandwidth.

4.6. The effects of the peak lifting factor χ

In this section, the effects of the peak lifting factor of JONSWAP spectrum on the interaction between focused wave groups and a vertical wall are investigated. Parameters for incident focused wave groups are shown in Table 6. The spectral density for different peak lifting factors is shown in Fig. 17. The peak value of spectral density is higher for larger values of peak lifting factors. It can be seen from Fig. 18 that the variation of peak lifting factors has little influences on the peak crest and adjacent trough of focused wave groups. However, with the increase of the peak lifting factor, the adjacent crest increases. This phenomenon may be better understood for limited conditions where χ approaches to infinity. In such conditions, much of the spectral energy is concentrated on the peak frequency, which is similar to a regular (monochromatic) wave. As a result, the adjacent crest is larger for larger value of peak lifting factors. As shown in Fig. 19, the peak crest of wave force time series is also insensitive to the peak lifting factor. For the trough, there is a slight increase with the increase of the peak lifting factor.

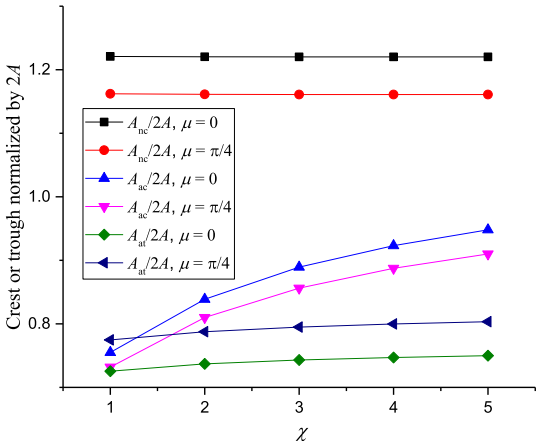

Fig. 18. Effects of peak lifting factors on the surface profile of focused wave groups interacting with a vertical wall.

5. Conclusions

In the present work, the interaction of nonlinear focused wave groups with a vertical wall is investigated based on the second order potential theory. The NewWave theory, which

Table 5
Parameters of focused wave groups of different frequency bandwidth.

Case	Frequency brandwidth, f_l-f_u (Hz)	Number of wave components, N	Water depth, h, (m)	Peak lifting factor, χ	Peak wavelength, k_p (m)	Peak crest, A (m)	Wave steepness, Ak_p
1	0.76–0.9	9	0.5	3.3	3	0.08	0.24
2	0.7–0.96	16	0.5	3.3	3	0.08	0.24
3	0.6–1.06	29	0.5	3.3	3	0.08	0.24
4	0.5–1.16	40	0.5	3.3	3	0.08	0.24
5	0.4–1.26	54	0.5	3.3	3	0.08	0.24
6	0.3–1.36	68	0.5	3.3	3	0.08	0.24

Table 6
Parameters of focused wave groups of different peak lifting factor.

Frequency brandwidth, f_l-f_u (Hz)	Number of wave components, N	Water depth, h, (m)	Peak lifting factor, χ	Peak wave number, k_p (m^{-1})	Peak crest, A (m)	Wave steepness, Ak_p
0.6–1.06	29	0.5	1–5	3	0.08	0.24

Please cite this article in press as: Sun, Y., Zhang, X., A second order analytical solution of focused wave group interacting with a vertical wall, International Journal of Naval Architecture and Ocean Engineering (2016), http://dx.doi.org/10.1016/j.ijnaoe.2016.09.002

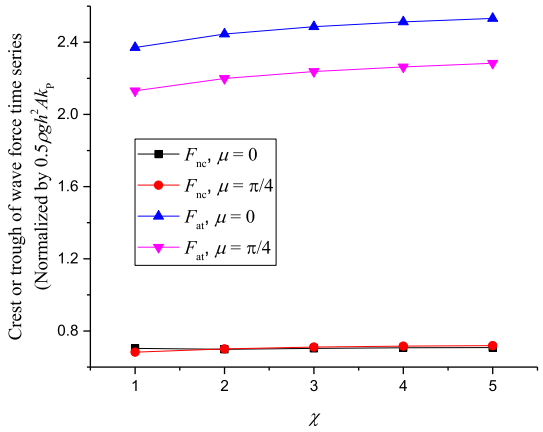

Fig. 19. Effects of peak lifting factors on wave forces exerted on the vertical wall.

represents the most probable surface elevation under a large crest, is adopted. The analytical solutions to the surface elevation and velocity potential are derived for focused wave groups interacting with a vertical wall. Also wave forces exerted by focused wave groups on the vertical wall are obtained, up to second order. After that, a parametric study is made on the interaction between focused wave groups and a vertical wall by considering the effects of angles of incidence, wave steepness, focal positions, water depth, frequency bandwidth and peak lifting factors. Some conclusions are drawn as follows.

1. The peak crest (trough) of surface profiles first decreases (increases) and then increases (decreases) with the increase of angles of incidence. However, the crest (trough) of wave forces rises (reduces) with angles of incidence.
2. As opposed to wave elevation, the peak crest (trough) of wave force time series reduces (increases) with the increase of wave steepness.
3. Empirical expressions are given for variation of surface profiles and wave forces with respect to wave steepness. The peak crest are more sensitive to wave steepness than the adjacent trough. The effects of wave steepness are more significant for smaller angles of incidence.
4. With the increase of the distance of the focal position from the vertical wall, the largest crest of surface elevation, although fluctuates, decreases gradually.
5. For surface elevation, with the reduction of water depth, the peak crest increases while the adjacent crest decreases. The adjacent trough first slightly increases and then decreases for shallower water depth. For wave force profile, both the peak crest and adjacent trough becomes larger for shallower water depth.
6. For focused wave groups interacting with a vertical wall, the frequency bandwidth has little influences on the peak crest of surface elevation or wave forces. However, both the adjacent crest and trough become smaller for larger frequency bandwidth.
7. Both the peak crest and adjacent trough of surface elevation and wave forces are insensitive to the variation of the peak lifting factor. However, the adjacent crest will increase with the increase of the peak lifting factor.

Acknowledgement

This work is supported by the IPRS, APA and Shell-UWA offshore engineering PhD research top-up scholarships in the University of Western Australia. These sources of support are gratefully acknowledged.

Appendix A.

Substituting Eqs. (32), (35)–(37) into Eq. (31), we get

$$F = \int_{-h}^{\eta} \left(P^{(0)} + P^{(1)} + P^{(2)}\right) dz = \int_{-h}^{0} \left(P^{(0)} + P^{(1)} + P^{(2)}\right) dz + \int_{0}^{\eta} \left(P^{(0)} + P^{(1)} + P^{(2)}\right) dz \tag{A1}$$

The hydrostatic force, $F^{(0)}$, is calculated as

$$F^{(0)} = \int_{-h}^{0} P^{(0)} dz = -\int_{-h}^{0} \rho g z dz = \frac{1}{2}\rho g h^2 \tag{A2}$$

The first order term of the force, $F^{(1)}$, is obtained by

$$F^{(1)} = \int_{-h}^{0} P^{(1)} dz = -\rho \int_{-h}^{0} \frac{\partial \phi^{(1)}}{\partial t} dz = \rho g \sum_{i=1}^{2N} \left[\frac{a_i}{|\vec{k}_i|} tanh\left(|\vec{k}_i| h\right) \cos \psi_i \right] \tag{A3}$$

The second order term of the force, $F^{(2)}$, is calculated using the following expression,

$$F^{(2)} = \int_{-h}^{0} P^{(2)} dz + \int_{0}^{\eta^{(1)}+\eta^{(2)}} \left(P^{(0)} + P^{(1)}\right) dz \tag{A4}$$

It should be noted that the first component at the right hand side (RHS) of Eq. (A4) is a second order term. However, the second component at RHS of Eq. (A4) includes both second and higher order terms. As a result, the higher order terms should be removed after calculation of the integration for the second component.

Please cite this article in press as: Sun, Y., Zhang, X., A second order analytical solution of focused wave group interacting with a vertical wall, International Journal of Naval Architecture and Ocean Engineering (2016), http://dx.doi.org/10.1016/j.ijnaoe.2016.09.002

$$\int_{-h}^{0} P^{(2)}dz = \int_{-h}^{0}\left\{-\rho\frac{\partial\phi^{(2)}}{\partial t}-\frac{1}{2}\rho\left[\left(\frac{\partial\phi^{(1)}}{\partial x}\right)^2+\left(\frac{\partial\phi^{(1)}}{\partial y}\right)^2+\left(\frac{\partial\phi^{(1)}}{\partial z}\right)^2\right]\right\}dz$$

$$=\rho\int_{-h}^{0}\sum_{i=1}^{2N}\left\{\frac{3}{4}a_i^2\omega_i^2\frac{\cosh\{2|\vec{k}_i|(z+h)\}}{\sinh^4\{|\vec{k}_i|h\}}\cos(2\psi_i)\right\}dz$$

$$+\rho\int_{-h}^{0}\sum_{i=1}^{2N-1}\sum_{j=i+1}^{2N}\left\{a_ia_jA_{ij}^{+}(\omega_i+\omega_j)\frac{\cosh\{|\vec{k}_i+\vec{k}_j|(z+h)\}}{\cosh\{|\vec{k}_i+\vec{k}_j|h\}}\cos(\psi_i+\psi_j)\right.$$

$$\left.+a_ia_jA_{ij}^{-}(\omega_i-\omega_j)\frac{\cosh\{|\vec{k}_i-\vec{k}_j|(z+h)\}}{\cosh\{|\vec{k}_i-\vec{k}_j|h\}}cos(\psi_i-\psi_j)\right\}dz$$

$$-\frac{1}{2}\rho\int_{-h}^{0}\left\{\sum_{i=1}^{2N}\left(a_i\frac{g}{\omega_i}|\vec{k}_i|\cos\mu_i\frac{\cosh\{|\vec{k}_i|(z+h)\}}{\cosh(|\vec{k}_i|h)}\cos\psi_i\right)\right\}^2dz$$

$$-\frac{1}{2}\rho\int_{-h}^{0}\left\{\sum_{i=1}^{2N}\left(a_i\frac{g}{\omega_i}|\vec{k}_i|\sin\mu_i\frac{\cosh\{|\vec{k}_i|(z+h)\}}{\cosh(|\vec{k}_i|h)}\cos\psi_i\right)\right\}^2dz$$

$$-\frac{1}{2}\rho\int_{-h}^{0}\left\{\sum_{i=1}^{2N}\left(a_i\frac{g}{\omega_i}|\vec{k}_i|\frac{sinh\{|\vec{k}_i|(z+h)\}}{\cosh(|\vec{k}_i|h)}\sin\psi_i\right)\right\}^2dz \tag{A5}$$

The final results of each term in the RHS of Eq. (A5) are given as follows.

a) the first term:

$$\rho\sum_{i=1}^{2N}\left\{\frac{3}{8}a_i^2\omega_i\frac{1}{|\vec{k}_i|}\frac{sinh(2|\vec{k}_i|h)}{\sinh^4(|\vec{k}_i|h)}\cos(2\psi_i)\right\} \tag{A6}$$

b) the second term:

$$\rho\sum_{i=1}^{2N-1}\sum_{j=i+1}^{2N}\left\{a_ia_jA_{ij}^{+}(\omega_i+\omega_j)\frac{1}{|\vec{k}_i+\vec{k}_j|}tanh(|\vec{k}_i+\vec{k}_j|h)\cos(\psi_i+\psi_j)+a_ia_jA_{ij}^{-}(\omega_i-\omega_j)\frac{1}{|\vec{k}_i-\vec{k}_j|}tanh(|\vec{k}_i-\vec{k}_j|h)cos(\psi_i-\psi_j)\right\} \tag{A7}$$

It should be noted that there are two limiting cases for the second term where the angle of incidence is 0 or π/2. For the case that the angle of incidence is 0, $|\vec{k}_i+\vec{k}_{i+N}|=0(i=1,2,\ldots,N)$. Similarly, for angle of incidence being π/2, $|\vec{k}_i-\vec{k}_{i+N}|=0(i=1,2,\ldots,N)$. When $|\vec{k}_i+\vec{k}_j|$ approaches to 0, $tanh(|\vec{k}_i+\vec{k}_j|h)$ approaches to $|\vec{k}_i+\vec{k}_j|h$. As a result, the ratio $\frac{1}{|\vec{k}_i+\vec{k}_j|}tanh(|\vec{k}_i+\vec{k}_j|h)$ approaches to h. Also we can obtain that $\frac{1}{|\vec{k}_i-\vec{k}_j|}tanh(|\vec{k}_i-\vec{k}_j|h)$ approaches to h as $|\vec{k}_i-\vec{k}_j|$ approaches to 0.

c) the third term:

For the case in which $i\neq j$ and $|i-j|\neq N$, the value of the third term in the RHS of Eq. (A5) is given as

$$-\rho\sum_{i=1}^{2N-1}\sum_{j=i+1,j\neq i+N}^{2N}\left\{a_ia_jg^2\frac{|\vec{k}_i||\vec{k}_j|}{\omega_i\omega_j}\cos\mu_i\cos\mu_j\cos\psi_i\cos\psi_j\times\left(\frac{|\vec{k}_i|}{|\vec{k}_i|^2-|\vec{k}_j|^2}\tanh(|\vec{k}_i|h)+\frac{|\vec{k}_j|}{|\vec{k}_j|^2-|\vec{k}_i|^2}\tanh(|\vec{k}_j|h)\right)\right\} \tag{A8}$$

For the case where $i=j$, the value of the third term in the RHS of Eq. (A5) is shown as

$$-\frac{1}{2}\rho\sum_{i=1}^{2N}\left\{a_i^2g^2\frac{|\vec{k}_i|^2}{\omega_i^2}\cos^2\mu_i\cos^2\psi_i\frac{1}{cosh^2|\vec{k}_i|h}\left(\frac{1}{2}h+\frac{1}{2|\vec{k}_i|}\cosh(|\vec{k}_i|h)\sinh(|\vec{k}_i|h)\right)\right\} \tag{A9}$$

For the case where $|i-j|=N$, the value of the third term in the RHS of Eq. (A5) is given as

$$-\rho\sum_{i=1}^{N}\left\{a_i a_{i+N} g^2 \frac{|\vec{k}_i||\vec{k}_{i+N}|}{\omega_i\omega_{i+N}}\cos\mu_i\cos\mu_{i+N}\cos\psi_i \times\cos\psi_{i+N}\frac{1}{cosh(|\vec{k}_i|h)cosh(|\vec{k}_{i+N}|h)}\left(\frac{1}{2}h+\frac{1}{2|\vec{k}_i|}\times\cosh(|\vec{k}_i|h)\sinh(|\vec{k}_i|h)\right)\right\} \tag{A10}$$

d) the fourth term

The calculation of the fourth term in the RHS of Eq. (A5) is similar as that of the third term and the results are given as follows,

$$-\rho\sum_{i=1}^{2N-1}\sum_{j=i+1,j\neq i+N}^{2N}\left\{a_i a_j g^2\frac{|\vec{k}_i||\vec{k}_j|}{\omega_i\omega_j}\sin\mu_i\sin\mu_j\cos\psi_i\cos\psi_j\left(\frac{|\vec{k}_i|}{|\vec{k}_i|^2-|\vec{k}_j|^2}\tanh(|\vec{k}_i|h)+\frac{|\vec{k}_j|}{|\vec{k}_j|^2-|\vec{k}_i|^2}\tanh(|\vec{k}_j|h)\right)\right\}$$
$$-\frac{1}{2}\rho\sum_{i=1}^{2N}\left\{a_i^2 g^2\frac{|\vec{k}_i|^2}{\omega_i^2}\sin^2\mu_i\cos^2\psi_i\frac{1}{cosh^2|\vec{k}_i|h}\left(\frac{1}{2}h+\frac{1}{2|\vec{k}_i|}\cosh(|\vec{k}_i|h)\sinh(|\vec{k}_i|h)\right)\right\}$$
$$-\rho\sum_{i=1}^{N}\left\{a_i a_{i+N} g^2\frac{|\vec{k}_i||\vec{k}_{i+N}|}{\omega_i\omega_{i+N}}\sin\mu_i\sin\mu_{i+N}\cos\psi_i\cos\psi_{i+N}\frac{1}{cosh(|\vec{k}_i|h)cosh(|\vec{k}_{i+N}|h)}\times\left(\frac{1}{2}h+\frac{1}{2|\vec{k}_i|}\cosh(|\vec{k}_i|h)\sinh(|\vec{k}_i|h)\right)\right\} \tag{A11}$$

e) the fifth term

The values of the fifth term in the RHS of Eq. (A5) is given as follows,

$$-\rho\sum_{i=1}^{2N-1}\sum_{j=i+1,j\neq i+N}^{2N}\left\{a_i a_j g^2\frac{|\vec{k}_i||\vec{k}_j|}{\omega_i\omega_j}\sin\psi_i\sin\psi_j\left(\frac{|\vec{k}_i|}{|\vec{k}_i|^2-|\vec{k}_j|^2}\tanh(|\vec{k}_j|h)+\frac{|\vec{k}_j|}{|\vec{k}_j|^2-|\vec{k}_i|^2}\tanh(|\vec{k}_i|h)\right)\right\}$$
$$-\frac{1}{2}\rho\sum_{i=1}^{2N}\left\{a_i^2 g^2\frac{|\vec{k}_i|^2}{\omega_i^2}\sin^2\psi_i\frac{1}{cosh^2|\vec{k}_i|h}\left(\frac{1}{2|\vec{k}_i|}\cosh(|\vec{k}_i|h)\sinh(|\vec{k}_i|h)-\frac{1}{2}h\right)\right\} \tag{A12}$$
$$-\rho\sum_{i=1}^{N}\left\{a_i a_{i+N} g^2\frac{|\vec{k}_i||\vec{k}_{i+N}|}{\omega_i\omega_{i+N}}\sin\psi_i\sin\psi_{i+N}\frac{1}{cosh(|\vec{k}_i|h)cosh(|\vec{k}_{i+N}|h)}\times\left(\frac{1}{2|\vec{k}_i|}\cosh(|\vec{k}_i|h)\sinh(|\vec{k}_i|h)-\frac{1}{2}h\right)\right\}$$

Please cite this article in press as: Sun, Y., Zhang, X., A second order analytical solution of focused wave group interacting with a vertical wall, International Journal of Naval Architecture and Ocean Engineering (2016), http://dx.doi.org/10.1016/j.ijnaoe.2016.09.002

Next we will calculate the value of the integration, $\int_0^{\eta^{(1)}+\eta^{(2)}} (P^{(0)}+P^{(1)})dz$, correct to second order.

$$\begin{aligned}\int_0^{\eta^{(1)}+\eta^{(2)}} P^{(0)}dz &= \int_0^{\eta^{(1)}+\eta^{(2)}} -\rho g z dz = -\frac{1}{2}\rho g\left(\eta^{(1)}+\eta^{(2)}\right)^2 \\ &= -\frac{1}{2}\rho g\left(\eta^{(1)}\right)^2 \\ &\quad + terms\ higher\ than\ \text{sec}\,ond\ order \\ &= -\frac{1}{2}\rho g\left(\sum_{i=1}^{2N} a_i \cos\psi_i\right)^2 \\ &\quad + terms\ higher\ than\ \text{sec}\,ond\ order \end{aligned} \tag{A13}$$

$$\begin{aligned}\int_0^{\eta^{(1)}+\eta^{(2)}} P^{(1)}dz &= -\rho \int_0^{\eta^{(1)}+\eta^{(2)}} \frac{\partial\phi^{(1)}}{\partial t}dz \\ &= \rho g \int_0^{\eta^{(1)}+\eta^{(2)}} \sum_{i=1}^{2N}\left[a_i \frac{\cosh\left\{\left|\overrightarrow{k}_i\right|(z+h)\right\}}{\cosh\left(\left|\overrightarrow{k}_i\right|h\right)}\cos\psi_i\right]dz \\ &= \rho g \sum_{i=1}^{2N}\left\{\frac{a_i}{\left|\overrightarrow{k}_i\right|\cosh\left(\left|\overrightarrow{k}_i\right|h\right)}\left|\overrightarrow{k}_i\right|\eta^{(1)}\cos\psi_i\right\} \\ &\quad + terms\ higher\ than\ \text{sec}\,ond\ order \end{aligned} \tag{A14}$$

References

Arena, F., 2005. On non-linear very large sea wave groups. Ocean Eng. 32 (11), 1311–1331.
Arena, F., Ascanelli, A., Nava, V., Pavone, D., Romolo, A., 2008. Three-dimensional nonlinear random wave groups in intermediate water depth. Coast. Eng. 55 (12), 1052–1061.
Baldock, T.E., Swan, C., 1996. Extreme waves in shallow and intermediate water depths. Coast. Eng. 27 (1), 21–46.
Boccotti, P., 1997a. A general theory of three-dimensional wave groups part I: the formal derivation. Ocean Eng. 24 (3), 265–280.
Boccotti, P., 1997b. A general theory of three-dimensional wave groups part II: interaction with a breakwater. Ocean Eng. 24 (3), 281–300.
Boccotti, P., Barbaro, G., Fiamma, V., Mannino, L., Rotta, A., 1993. An experiment at sea on the reflection of the wind waves. Ocean Eng. 20 (5), 493–507.
Dalzell, J.F., 1999. A note on finite depth second-order wave–wave interactions. Appl. Ocean Res. 21 (3), 105–111.
Edge, R.D., Walters, G., 1964. The period of standing gravity waves of largest amplitude on water. J. Geophys. Res. 69 (8), 1674–1675.
Fedele, F., Arena, F., 2005. Weakly nonlinear statistics of high random waves. Phys. Fluids 17 (2), 026601 (1994-present).
Fultz, D., 1962. An experimental note on finite-amplitude standing gravity waves. J. Fluid Mech. 13 (02), 193–212.
Goda, Y., 1967. The fourth order approximation to the pressure of standing waves. Coast. Eng. Jpn. 10 (1).
Hasselmann, K., Barnett, T.P., Bouws, E., Carlson, H., Cartwright, D.E., Enke, K., ..., Meerburg, A., 1973. Measurements of Wind-wave Growth and Swell Decay during the Joint North Sea Wave Project (JONSWAP). Deutches Hydrographisches Institut.
Newman, J.N., 1977. Marine hydrodynamics. MIT press.
Penney, W.G., Price, A.T., 1952. Part II. Finite periodic stationary gravity waves in a perfect liquid. Philos. Trans. R. Soc. Lond. A Math. Phys. Eng. Sci. 244 (882), 254–284.
Prabhakar, V., Sundar, V., 2001. Standing wave pressures on walls. Ocean Eng. 28 (5), 439–455.
Rayleigh, L., 1915. Deep water waves, progressive or stationary, to the third order of approximation. Proc. R. Soc. Lond. Ser. A Contain. Pap. Math. Phys. Charact. 91 (629), 345–353.
Romolo, A., Arena, F., 2008. Mechanics of nonlinear random wave groups interacting with a vertical wall. Phys. Fluids 20 (3), 036604, 1994-present.
Romolo, A., Arena, F., 2013. Three-dimensional non-linear standing wave groups: formal derivation and experimental verification. Int. J. Non-Linear Mech. 57, 220–239.
Romolo, A., Arena, F., Laface, V., 2014. A generalized approach to the mechanics of three-dimensional nonlinear ocean waves. Probab. Eng. Mech. 35, 96–107.
Sharma, J.N., Dean, R.G., 1981. Second-order directional seas and associated wave forces. Soc. Pet. Eng. J. 21 (01), 129–140.
Sriram, V., Schlurmann, T., Schimmels, S., 2015. Focused wave evolution using linear and second order wavemaker theory. Appl. Ocean Res. 53, 279–296.
Tadjbakhsh, I., Keller, J.B., 1960. Standing surface waves of finite amplitude. J. Fluid Mech. 8 (03), 442–451.
Taylor, G., 1953 June. An experimental study of standing waves. Proc. R. Soc. Lond. a: Math. Phys. Eng. Sci. 218 (1132), 44–59 (The Royal Society).
Tromans, P.S., Anaturk, A.R., Hagemeijer, P., 1991 January. A new model for the kinematics of large ocean waves-application as a design wave. In: The First International Offshore and Polar Engineering Conference. International Society of Offshore and Polar Engineers.
Walker, D.A.G., Taylor, P.H., Taylor, R.E., 2004. The shape of large surface waves on the open sea and the Draupner New Year wave. Appl. Ocean Res. 26 (3), 73–83.

Please cite this article in press as: Sun, Y., Zhang, X., A second order analytical solution of focused wave group interacting with a vertical wall, International Journal of Naval Architecture and Ocean Engineering (2016), http://dx.doi.org/10.1016/j.ijnaoe.2016.09.002